



PAPER • OPEN ACCESS

Co *K*-edge magnetic circular dichroism across the spin state transition in LaCoO₃ single crystal

To cite this article: V Efimov *et al* 2016 *J. Phys.: Conf. Ser.* **712** 012111

View the [article online](#) for updates and enhancements.

You may also like

- [Cathode Performance of Co-Doped Li₂O with Specific Capacity \(400 mAh/g\) Enhanced by Vinylene Carbonate](#)
Hiroaki Kobayashi, Mitsuhiro Hibino, Yuki Kubota *et al.*
- [Molecular Distributions of the Protostellar Envelope and the Outflow of IRAS 15398–3359: Principal Component Analysis](#)
Yuki Okoda, Yoko Oya, Nami Sakai *et al.*
- [Evolution of local structure and superconductivity in CaFe₂As₂](#)
Ram Prakash Pandeya, Arindam Pramanik, Anup Pradhan Sakhya *et al.*

The Electrochemical Society
Advancing solid state & electrochemical science & technology

ECS UNITED

247th ECS Meeting
Montréal, Canada
May 18-22, 2025
Palais des Congrès de Montréal

Showcase your science!

Abstracts due December 6th

Co *K*-edge magnetic circular dichroism across the spin state transition in LaCoO₃ single crystal

V Efimov¹, A Ignatov², I O Troyanchuk³, V V Sikolenko^{1,4}, A. Rogalev⁵, F. Wilhelm⁵, E Efimova¹, S I Tiutiunnikov¹, D Karpinsky³, V Kriventsov⁶, E Yakimchuk⁶, S Molodtsov⁷, P Sainctavit⁸ and D Prabhakaran⁹

¹ Joint Institute for Nuclear Research, 141980 Dubna, Russia

² Oak Ridge National Laboratory, Oak Ridge, TN 37831, USA

³ Scientific-Practical Material Research Center NAS Belarus, 220072 Minsk, Belarus

⁴ REC "Functional nanomaterials" Immanuel Kant Baltic Federal University, 236041 Kaliningrad, Russia

⁵ European Synchrotron Radiation Facility, BP 220, 38043 Grenoble, France

⁶ Borekov Institute of Catalysis SB RAS, 630090 Novosibirsk, Russia

⁷ European XFEL GmbH, Albert-Einstein-Ring 19, 22761 Hamburg, Germany

⁸ Institut de minéralogie et de physique des milieux condensés CNRS F-75012, France

⁹ Department of Physics, University of Oxford, OX1 3PU, Oxford, Great Britain

E-mail: efimovvv2006@mail.ru

Abstract. We report on Co *K*-edge x-ray magnetic circular dichroism (XMCD) measurements of LaCoO₃ single crystal in temperature range from 5 to 300 K and external magnetic field of 17 T. The response consists of pre-edge (at 7712 eV) and bi-polar peak (up at 7727, down at 7731 eV) with amplitudes, respectively, less than 10⁻³ and 10⁻² of the Co *K*-edge jump. Using the sum rule the orbital magnetic moment of 4*p* Co is evaluated. Its temperature dependence reaches a maximum of $(2.7 \pm 0.9) \times 10^{-3} \mu_B$ at 120 K, following the trend for the total magnetic moment on the Co obtained from the superconducting quantum interference device measurements. However, on warming from 25 to 120 K, the orbital magnetic moment of the 4*p* Co doubles while total magnetic moment of Co increases 10 times. First principle calculations are in order to relate the Co *K*-edge XMCD results to the orbital and spin moment of 3*d* Co.

1. Introduction

A perovskite LaCoO₃ exhibits variety of physical properties [1-11]. At low temperature the Co³⁺ ion is in the low-spin state (LS; $t_{2g}^6 e_g^0$, $S = 0$). Thermal activation of LS state into intermediate-spin state (IS; $t_{2g}^5 e_g^1$, $S = 1$) or high-spin state (HS; $t_{2g}^4 e_g^2$, $S = 2$) is observed in the temperature interval from 40 to 120 K [3-10]. Korotin *et. al.* [2] argued that IS state is stabilized by strong 3*d*(Co)-2*p*(O) hybridization. Currently, there are plenty experimental works supporting either LS-IS [2-6] or LS-HS [7-9] scenario. Co *L*_{2,3}-edges x-ray magnetic circular dichroism (XMCD) accompanied by theoretical calculations for the CoO₆ cluster [9] have shown that the spin-state transition in LaCoO₃ can be well described by thermal excitation from LS ground state into a triply degenerated HS state. However, bonds breaking, strains, and oxygen vacancies on the surface can modify spin state of the Co ion [10, 11]. The present experimental work is undertaken to provide an essentially bulk probe of Co spin states by using a hard X-ray XMCD at the Co *K*-edge.



2. Experimental

LaCoO₃ single crystal (~ 10 mm in diameter and ~10 cm long) were grown by the floating zone method. The sample were cut in pieces and characterized using x-ray diffraction, EXAFS [12], and superconducting quantum interference device (SQUID) magnetometry. The X-ray absorption near edge spectra (XANES) and X-ray magnetic circular dichroism (XMCD) measurements were performed on beamline ID12 of the European Synchrotron Radiation Facility at Grenoble. All Co K-edge absorption spectra were recorded in total fluorescence yield (TFY) measurements for normal incidence (a backscattering geometry) of the x-ray beam using 98% circularly polarized X-rays. XMCD measurements were performed using 98% circularly polarized x-rays. The signal was recorded from the difference in absorption for parallel and antiparallel alignments of the X-ray helicity pseudovector with respect to an external magnetic field of 17 T, applied along the beam direction. The x-ray helicity and the external magnetic field direction were alternately flipped to minimize experimental artifacts. Six to eight measurements were averaged in order to improve the signal-to-noise ratio.

3. Results and discussion

The Co *K* edge absorption and XMCD spectra measured at 5, 25, 60, 120, 150, and 300 K are shown in Fig. 1. The XANES consists of two areas: the pre-edge (7709-7716 eV) due to a quadruple transition from *1s* to unoccupied *3d*, and the main edge (7716-7740 eV) due to a dipole transition from *1s* to unoccupied *4p* -states. The *3d* of Co are split into *t*_{2g} and *e*_g by the crystal field that clearly seen as a doublet P1- P2. Peaks A, B, and C (at ~7720, 7727, and 7738 eV, respectively) are the best described in the formalism of multiple scattering (MS) of the photoelectron in the cluster of 40-60 atoms centered on the Co absorption site: The major peak B is formed by scattering from the first coordination shell comprised of six oxygen atoms. The peaks A and C are shaped by MS of the photoelectron from more distant coordination shells.

The Co *K*-edge XMCD is driven by orbital polarization of unoccupied *4p* states coupled to spin polarization of the same *4p* by spin-orbit interaction, ξ_{4p} . The spin polarization of *4p* occurs due to hybridization of those states with essentially spin-polarized *3d* band. The XMCD manifests itself as a weak pre-edge doublet and a bi-polar feature (peak "up" at ~7727 eV followed by peak "down" at ~7731 eV) located in vicinity of the major absorption peak B. In the external magnetic field of 17 T the amplitudes of the pre-edge and the bi-polar feature do not exceed 10⁻³ and 10⁻² of the Co *K*-edge jump. XMCD signal has been successfully measured due to high signal-to-noise ratio, good stability of the beamline, and accurate energy reference. Contrary to ferromagnetics, metal Co, for instance, where the XMCD signal is given by single peak, the observed bi-polar structure is typical for paramagnetic Co, i.e. Co doped ZnO [13] and antiferromagnetic Co, i.e. Co doped LaMnO₃ [14].

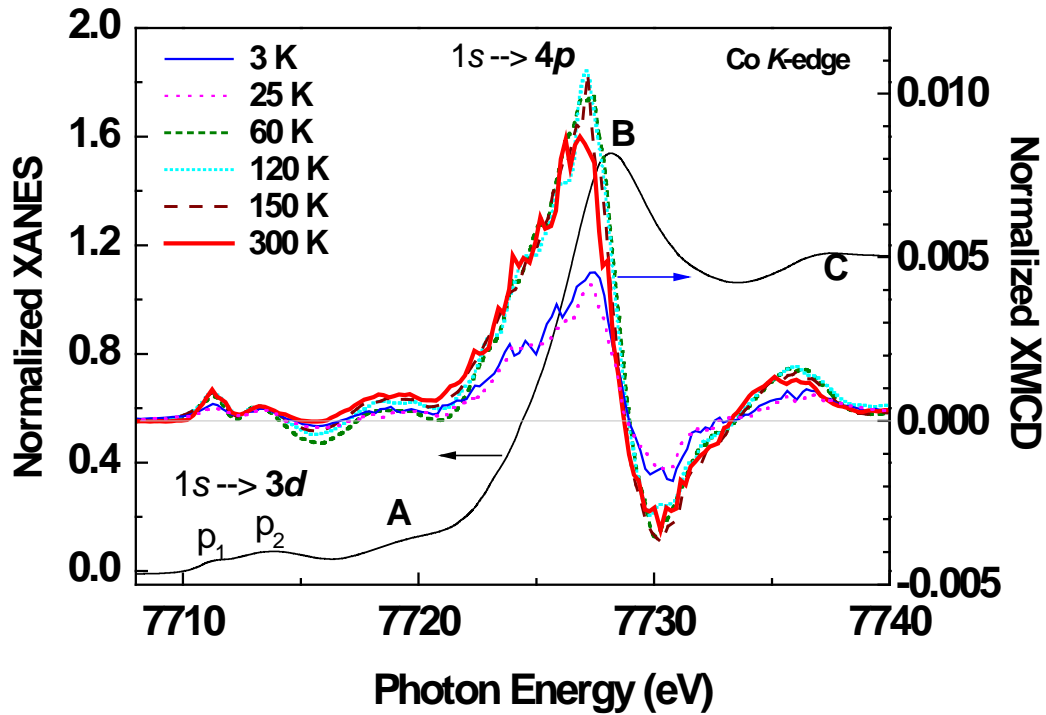


Fig. 1: Co *K*-edge absorption and temperature-dependent XMCD spectra of LaCoO₃ single crystal, measured under external magnetic field of 17 Tesla applied along the incident beam (that is also the *c*-axis). The background was subtracted and the absorption spectrum was normalized to a unit jump at 50-60 eV above the edge. The XMCD is given as a fraction of the absorption edge jump.

By application of a sum rule [15] the integrated *K*-edge XMCD intensity can be related to the orbital magnetic moment of *4p*, $\langle L_z \rangle_{4p}$ as per one Co atom:

$$\langle L_z \rangle_{4p} = - (6 - n_{4p}) \cdot (2I_{\text{XMCD}} / 3I_{\text{XANES}})$$

where n_{4p} is the electron count in the *4p*, I_{XMCD} and I_{XANES} are the integrated over the range from 7716 to 7750 eV XMCD and XANES signals. The low limit cut off negligible contribution from *p*-states over the pre-edge. The upper limit aims at separating atomic from continuum contributions. Uncertainties in selection of n_{4p} that were taken equal to 1.0 and selection of the upper integration limit propagates to 20-30% uncertainty in the evaluated $\langle L_z \rangle_{4p}$.

The obtained orbital moments for all measured temperatures are shown in Fig 2 along with total magnetic moments per Co ion derived from our SQUID magnetization measurements, though in slightly smaller applied field. Clearly, the $\langle L_z \rangle_{4p}$ following the trend for the total magnetic moment on the Co ion. However, on warming from 25 to 120 K, the orbital magnetic moment of the *4p* Co doubles while total magnetic moment of Co increases 10 times. First principle calculations are in order to relate the Co *K*-edge XMCD results to the orbital and spin moment of *3d* Co.

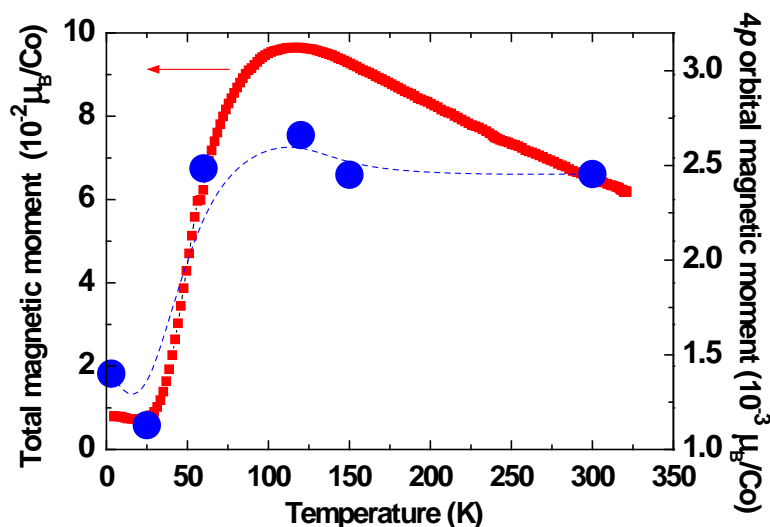


Fig. 2. Comparison of 4p orbital magnetic moment per Co derived from XMCD sum rule with total magnetic moment per Co ion obtained from SQUID magnetization measurements as a function of the temperature. The XMCD and SQUID data were collected in applied magnetic fields of 17 and 14 T, respectively. Uncertainties for 4p orbital magnetic moment are ~ 20-30% (refer to the text for details).

Acknowledgments

This work was supported by RFBR Grants No. 15-32-50367_mol_np and No. 13-02-00699_a.

References

- [1] J. B. Goodenough, *J. Phys. Chem. Solids* **6**, 287 (1958)
- [2] M. A. Korotin, S. Y. Ezhov, I. V. Solovyev, V. I. Anisimov, D. I. Khomskii, and G. A. Sawatzky, *Phys. Rev. B* **54**, 5309 (1996)
- [3] P. G. Radaelli and S.-W. Cheong, *Phys. Rev. B* **66**, 094408 (2002).
- [4] K. Asai, A. Yoneda, O. Yokokura, J. M. Tranquada, G. Shirane, and K. Kohn, *J. Phys. Soc. Jpn.* **67**, 290 (1998)
- [5] C. Zobel, M. Kriener, D. Bruns, J. Baier, M. Gruninger, T. Lorenz, P. Reutler, and A. Revcolevschi, *Phys. Rev. B* **66**, 020402 (2002)
- [6] R. F. Klie, J. C. Zheng, Y. Zhu, M. Varela, J. Wu, and C. Leighton, *Phys. Rev. Lett.* **99**, 047203 (2007)
- [7] A. Podlesnyak, S. Streule, J. Mesot, M. Medarde, E. Pomjakushina, K. Conder, A. Tanaka, M. W. Haverkort, and D. I. Khomskii, *Phys. Rev. Lett.* **97**, 247208 (2006)
- [8] S. Noguchi, S. Kawamata, K. Okuda, H. Nojiri, M. Motokawa, *Phys. Rev. B* **66**, 094404 (2002)
- [9] M. W. Haverkort, Z. Hu, J. C. Cezar, T. Burnus, H. Hartmann, M. Reuther, C. Zobel, T. Lorenz, A. Tanaka, N. B. Brookes, H. H. Hsieh, H.-J. Lin, C. T. Chen, and L. H. Tjeng, *Phys. Rev. Lett.* **97**, 176405 (2006)
- [10] J.-Q. Yan, J.-S. Zhou, and J. B. Goodenough, *Phys. Rev. B* **70**, 014402 (2004)
- [11] I. O. Troyanchuk, M. V. Bushinsky, and L. S. Lobanovsky, *J. Appl. Phys.* **114**, 213910 (2013).
- [12] Sikolenko V, Troyanchuk I, Efimov V, Efimova E, Karpinsky D, Sakura P, Zaharko O, Ignatov A, Aquilanti D, Selutin A, Shmakov A and Prabhakaran D, *J. Phys. Conference Series*, in press.
- [13] Ney A, Ollefs K, Ye S, Kammermeier T, Ney V, Kaspar T C, Chambers S A, Wilhelm A F, and Rogalev A, 2008 *Phys. Rev. Lett.* **100**, 157201
- [14] Burnus T, Hu Z, Hsieh H H, Joly V L J, Joy P A, Haverkort M W, Hua Wu, A. Tanaka A, Lin H J, Chen C T, and Tjeng L H, 2008 *Phys. Rev. B* **77** 125124
- [15] Guo G P, 1998 *Phys. Rev. B* **57** 10295.